AIMS Materials Science, 3(3): 916-926.
DOI: 10.3934/matersci.2016.3.916
Received: 12 May 2016
Accepted: 05 July 2016
Published: 18 July 2016

http://www.aimspress.com/journal/Materials

Research article

Microstructural and magnetic properties of YBCO nanorods: synthesized by template growth method

S. Pavan Kumar Naik [1] and P. Missak Swarup Raju [2,*]

[1] School of Physics, University of Hyderabad, Hyderabad-500046, India
[2] Department of Physics, GITAM University, Hyderabad, India-502329

* **Correspondence:** Email: swarupraj@gmail.com; Tel: +91-40-23134365.

Abstract: Superconductivity in a low dimensional structure is an interesting phenomenon both from fundamental and application point of view. The present study proposes a novel method of fabricating single crystalline $YBa_2Cu_3O_{7-\delta}$ (YBCO/Y123) nanorods from the nitrate solution containing Yttrium (Y), Barium (Ba) and copper (Cu) ions in stoicheometric proportion to that of Y123. The nitrate solution was soaked into cellulose and then was heated to a phase formation temperature of 880 ^oC with a dwell of 6 and 24 hours followed by oxygenation for 100 hours at 460 ^oC. Fine particles of YBCO, sintered together to form long (>100 μm) thread like structure with a diameter of ~2 μm were observed. At higher magnification nano-rods with ~ 50–100 nm diameters and length of ~500 nm were observed for 24 hours heat treated sample. Selective area electron diffraction was done on these nanorods and was compared with the simulated pattern of YBCO. A broad diamagnetic, transition in magnetic susceptibility below 90 K indicates the presence of superconductivity. M-H loops recorded at 77 K on these samples indicate superconducting behavior at low fields and paramagnetic behavior at high fields. M-H loops above superconducting transition (90 K–300 K) unveil the ferromagnetism in these samples.

Keywords: nanorods; superconductors; microstructure; magnetic properties; nanostructures; TEM

1. Introduction

Nano-rods are quantum confined, and they exhibit distinct properties that are not accessible to their bulk material counterparts [1]. In the quantum confined regime, physical properties can be manipulated by merely changing the size and shape of the materials [2]. Recently, single-crystalline

whiskers have drawn a lot of attention because of their exceptional features such as perfect crystallinity, in particular, the absence of dislocations within extremely small cross sections. Superconducting nano-rods with high critical temperature (T_c) are useful for the fabrication of electronic devices using intrinsic Josephson effects and related phenomena, such as Josephson plasma oscillations [3]. These junctions show a homogeneous multi-branched structure with voltage gaps of several tens of millivolts in I-V characteristics [3–6]. The studies suggest that the junctions have the potential to become prospective candidates for electronic devices with high-frequency terahertz (THz) band.

$YBa_2Cu_3O_{7-\delta}$ (YBCO) superconductors have an advantage over Bi-based superconductors for the THz frequency applications, because of its higher critical current density (J_c) particularly at 77 K. However, there are no reports of successful fabrication of YBCO single crystal with nanometric dimensions [7]. Can superconductivity survive in (quasi)-1D systems, or do fluctuations suppress phase coherence thus disrupting any super current? The answers to such questions are of interest from fundamental as well as practical interest. On one hand, investigations on this subject will help to uncover novel physics and shed more light on the crucial role of superconducting fluctuations in the 1D wire. On the other hand, rapidly progressing miniaturization of nanodevices opens new horizons for applications of superconductivity at nano-scales such as superconducting nanocircuits [8].

Magnetism in superconductivity was first considered by Ginzburg [9] who proposed that the existence of ferromagnetism is possible only if the internal magnetic moment is smaller than the thermodynamic critical field of the superconductivity. The discovery of UGe_2 system confirmed the coexistence of both the superconductivity and ferromagnetism which otherwise believed as incompatible phenomena [10]. Gasima et al. [11] established the coexistence of ferromagnetism and superconductivity in nano-sized powders of YBCO at 4.2 K. Afterward room temperature ferromagnetism in YBCO system is reported by many groups [12–15]. Ferromagnetism in YBCO nanoparticles is believed to be the result of oxygen vacancies which are created at the surface [16,17]. The size effect on the superconducting and magnetic properties of the nanometric YBCO particles were studied and reported by Hasnain et al. [18].

There are some reports on the preparation methods of nano YBCO, and the existence of superconductivity and ferromagnetism was observed in most of the cases. Mainly the preparation is carried out by citrate pyrolysis [18,19], citrate-gel method [20], melting process [11] and solid state route through sintering [21]. The sizes of YBCO nanoparticles in these reports were mostly estimated from the XRD line broadening using the Scherer formula. The sizes of the YBCO obtained in the above method are of the order of 50–500 nm. Most often, Pulsed Laser Ablation and thermal decomposition routes have yielded YBCO nano-rods, the focus of the studies were microstructure and to some extent, the crystal structure of these nanorods, but not their superconducting properties [19,22].

We report a novel approach for the synthesis of single crystal nanorods of YBCO with uniform diameters as small as 50 nm and lengths up to 500 nm. This route offers the synthesis of YBCO nano-rods on its grains, but one has to optimize the process conditions in order to obtain fine nano YBCO of desired length and diameter for practical applications. Micro-structural, magnetization measurements with respect to temperature (77 K to room temperature) and magnetic field were carried out. XRD and selective area electron diffraction (SAED) on single nano YBCO rod were carried out to confirm the structural details and compared with simulated SAED patterns.

2. Materials and Method

Y_2O_3 (Rare Earth make), $BaCO_3$ and CuO (E-Merck make) of 99.99% purity, were taken in Y123 stoichiometric ratio and were dissolved in HNO_3 (E-Merck make) with continual stirring for 1 hour to form a uniform solution. The solution was then introduced into cellulose and was then heat treated in a recrystallized Al_2O_3 crucible to 880 ^oC with a dwell time of 6 and 24 hours respectively. The samples will be referred to as Y123C-6 and Y123C-24 in the discussion for convenience. Thus formed powder was then oxygenated at 460 ^oC for 100 hours in order to obtain the YBCO superconducting phase. Microstructural characterization was carried out employing a Field Emission Scanning Electron Microscopy (FESEM; Zeiss-make Ultra 55 model). X-ray diffraction (XRD) patterns are recorded using Cu K_α as the X-ray source (λ = 1.5405 Å); Bruker's AXS Model D8 Advance System was used to carry out the XRD measurement. Selective Area Electron Diffraction (SAED) measurements were carried out for single nano Y123C-24 rod and compared with simulated SAED pattern for superconducting $YBa_2Cu_3O_{6.97}$ composition using WebEMAPS [23]. Magnetic hysteresis loops were recorded using a Physical Property Measurement System (PPMS; Quantum Design) at low temperature and VSM (lakeshore 665) upto room temperature.

3. Results and Discussion

In earlier reports [11,18–22] on nano YBCO (50–500 nm), the primary emphasis was synthesis, but none provided insight on the correlation between superconductivity and ferromagnetism with the size of nano YBCO. Zuo et al. [23] reported the fabrication of 500 nm YBCO in combustion reaction method using citrate precursors but formed nanoparticles, but not rods. Zhang et al., [22] fabricated 18–96 nm sized quasi-one-dimensional (Q1D) YBCO rods grown on YBCO grains by LASER ablation method through oxide-assisted growth mechanism, which is promising but expensive method. It was also reported that other factors, such as the selection of the starting reactants, techniques employed and the calcination temperature and procedures followed play an important role in the phase formation and the characteristics of fabricated samples [19,24]. Most of the reported compounds were synthesized by solid state reaction of Y_2O_3 and CuO with $BaCO_3$ [25,26,27] or BaO_2 [24,28,29] and followed by prolonged calcination to decompose carbonates.

The present work brings forth a novel and efficient method of preparation for YBCO nanorods. It has been observed in literature that solution based methods yield single-phase YBCO composites because of stoichiometric distribution of elements at the atomic level. In this work, we have adopted solution based method along with template growth technique to obtain YBCO nano-rods. Cellulose was used as a template for nanorod formation as it has a fine thread-like morphology and can be removed completely upon heating without any undesired residue. If the cellulose is soaked in the clear nitrate solution, containing a stoichiometric proportion of Y, Ba, Cu atoms to form YBCO, it is expected that fine thread like YBCO structure can be formed when heated at phase forming temperature. It is also known that lowering the sintering temperature restricts the grain growth [18], but can lead to the formation of secondary phases. Hence, the sintering temperature was chosen in such a way that single phase YBCO can be formed without much grain growth. Cellulose, soaked in above said nitrate solution, was heat treated at 880 ^oC in order to restrict the grain growth as well as to get YBCO phase without any residual phases like $BaCO_3$, etc. [18]. Sintering duration also influences the uniformity in phase formation and growth. Hence, two different sintering durations (6 hours and 24 hours) were chosen for the present study.

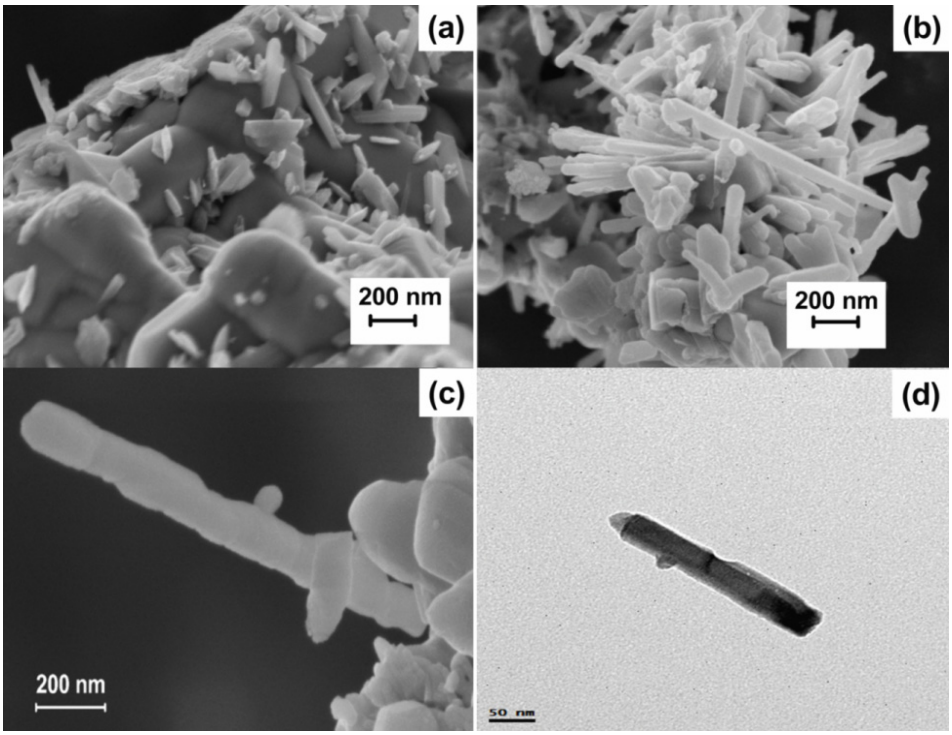

Figure 1. FESEM images obtained on Y123C-6 and Y123C-24 at a magnification of 100 kX shown in (a) and (b) respectively. FESEM image of single nanorod of Y123C-24 recorded at 150 kX is shown in (c). TEM micrograph of a nanorod found in the YBCOC-24 sample is shown in (d).

Fine rod-like structures grown on the YBCO particles was observed under FESEM micrographs obtained at 100 kX as shown in Figure 1. The widths of these nanorods are around 100 nm. Longer rods were observed in Y123C-24 compared to Y123C-6. In Y123C-6, nano sprout like structure appears on YBCO particles (Figure 1.(a)) and as time progresses these sprouts grow into nanorod (Figure 1. (b)).

The lengths of the observed nano-rods on YBCO particle have increased with prolonged sintering duration. FESEM (at 150 kX magnification) and the TEM image of single nano Y123C-24 rod are shown in Figure 1 (c) and (d) respectively and the lengths of the rods are of the order of 500 nm to 200 nm. The size and morphology of YBCO nanorods observed in Y123C-24 are comparable to the earlier reports. But the present synthesis method is straightforward, reproducible and cost effective as compared to the reports available in literature.

YBCO samples were oxygenated at 460 ^{o}C for 100 hours to obtain the orthogonal superconducting phase. X-ray diffractograms for oxygenated Y123C-6 and Y123C-24 samples are shown in Figure 2. The observed peaks in these samples can be indexed to an orthorhombic Y123 phase with JCPDS card numbers 895842 and 893455 along with minor peaks corresponding to Ba-Cu-O phases such as $BaCuO_2$, $Ba_2Cu_3O_{5.9,}$ and $BaCu_2O_2$. As discussed in the literature [18], heat treatments above 860 ^{o}C should eliminate $BaCO_3$ phase but in the present study, only YBCO crystalline phase is observed along with traces of Ba-Cu-O_3 phases. The extended sintering for Y123C-24 has suppressed Ba-Cu-O phase which is present in Y123C-6 to a considerable amount and

favored enhancement of crystallinity of YBCO phase. The peaks are broad indicating the presence of nanocrystalline phases in these samples.

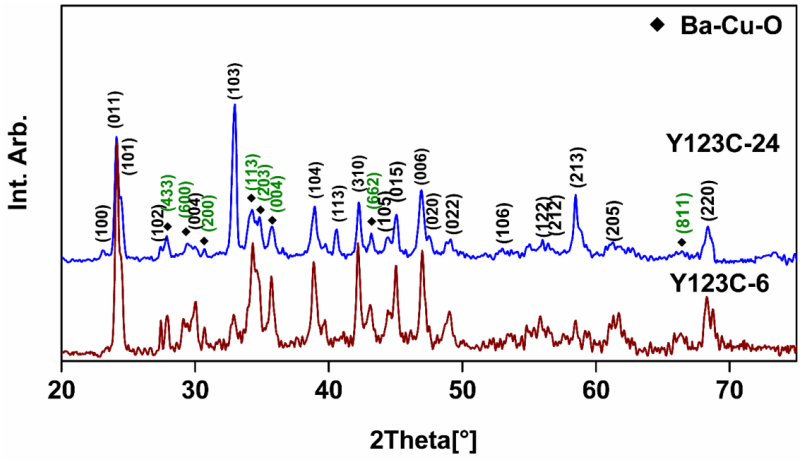

Figure 2. XRD patterns of Y123C-6 and Y123C-24; the peaks are indexed to Y123 phase. Ba-Cu-O phase fraction is found to be more in Y123C-6. ♦ symbol represents the peaks corresponding to Ba-Cu-O phases.

TEM provides a unique method to probe the phase transitions on a local scale and also provides detailed structural information of phases present. Indexed SAED pattern corresponding to Y123C-24 sample (on Figure 1 (d)) is shown in Figure 3 (a) is taken along the [001] zone axis. Y123C-24 crystal gave a perfect single crystalline SAED pattern which can be indexed to the orthorhombic Pmmm space group. For the orthorhombic Pmmm symmetry, the simulation was done for $YBa_2Cu_3O_{6.97}$ superconducting phase with [001] zone axis using Web Electron Microscopy Applications Software (WebEMAPS) [29] and provided in Figure 3 (b). The diffraction patterns taken on the nano YBCO nano-rod and the simulated patterns were compared, and reflections are in good agreement.

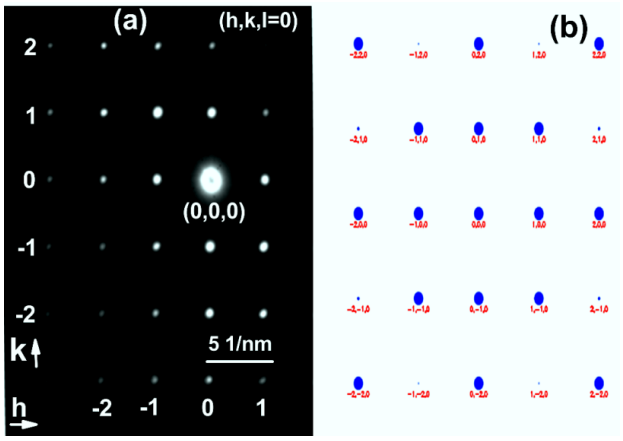

Figure 3. (a) TEM diffraction pattern of a Y123C-24 single crystal having [001] growth direction and (b) represents the corresponding simulated electron diffraction pattern tilted along the [001] axis.

In order to ascertain superconductivity in the samples, magnetization versus temperature (M-T) was measured and the plots are shown in Figure 4. YBCO particles were stuck together with an adhesive (free from any magnetic impurities) in order to arrest relative movement of the particles while performing the measurement. It was observed that the diamagnetic transition for both the samples occur below 90 K, but the transition is broad which may be due to the nanosize of the YBCO rods. Critical temperatures in superconducting nanoparticles are suppressed compared to bulk counterparts because of the fluctuations at smaller dimensions and loss of coordination at the surface. Hasnain et al. [18] have observed that with decreasing size of the YBCO particles ferromagnetic and paramagnetic contribution increases at room temperature while the superconducting transition temperature decreases.

Broadening of transition widths usually depends on the oxygen content i.e. δ in the $YBa_2Cu_3O_{7-\delta}$ system, with increasing loss of oxygen the transition temperature can decrease from 93 K to 30 K [30] while above δ~ 0.7 in the YBCO loss their superconducting properties. Other factors contributing to the broad transition are the inhomogeneous structures of the material, i.e., different regions of the sample have a slightly different response at the same time and the presence of the ferromagnetic phase in the system. It was also pointed out by Little [31] that quasi-one-dimensional wires made up of a superconducting material can acquire a finite resistance below T_c of a bulk material due thermally activated phase slips (TAPS).The thermo-activated phase slips (near T_c) widen the transition region. But since the superconducting nanowires are not ideal 1D, most of the nanowires still show zero resistance far below T_c. Sometimes the loss of zero resistance may lead due to the large disorder in nanowires. Sufficiently, thin superconducting wires can acquire non-zero resistance even below T_c due to fluctuations of the superconducting order parameter [31]. It is a well-known experimental fact that the T_c of thin superconducting films frequently differs from the bulk samples [32]. A similar pattern is also observed in metallic nanostructures. In crystalline Bi, Pb, indium, aluminum and zinc nanowires T_c increases with decreasing characteristic dimension [33–39]. On the contrary, in lead, niobium and MoGe an opposite tendency is observed [40–44]. No noticeable variations of T_c were detected in tin nanowires [45–49]. The origin of this phenomenon is not clear, because even chemically pure nanostructures cannot be considered as sufficiently homogeneous as soon as the size dependence of the T_c comes into play. One should study atomically homogeneous systems as single crystalline nanorods [50]. Unfortunately, modern nanotechnology has a limitation on growth of high-quality quasi-1D single crystals of arbitrary diameter made up of all materials that are interesting for various reasons.

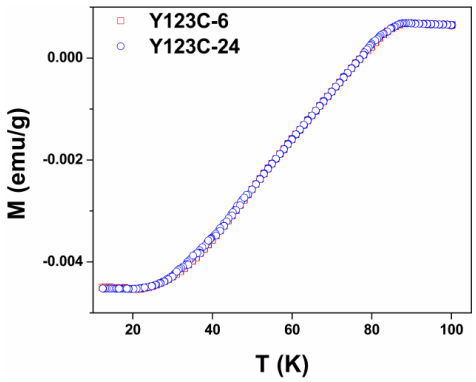

Figure 4. Temperature-dependence of magnetization curves of the Y123C-6 and Y123C-24 show a broad diamagnetic transition for both the samples.

Magnetic hysteresis loops obtained on Y123C-6, and Y123C-24 samples at 77 K are shown in Figure 5. Negative magnetic moment of the particle with increasing fields up to 500 Oe indicates the presence of superconductivity. The magnetization beyond 500 Oe is dominantly paramagnetic in nature because the YBCO nano-rods are very fine and separated by large free spaces, the supercurrent generated within the YBCO nanorods due to applied field beyond 500 Oe is sufficient to destroy the superconductivity. Interestingly the M-H loop is not closed even though they are traced to up to 3 T field as can be seen in the inserts in Figure 5 (a). A different approach needs to be set up to calculate critical current densities on these nanorods. It was also observed that the value of H_c1 for Y123C-6 (~ 160 Oe) is less than Y123C-24 (~400 Oe) and the enlarged portion of MH curve at 77 K which indicates the diamagnetic behavior, as shown in Figure 5 (b).

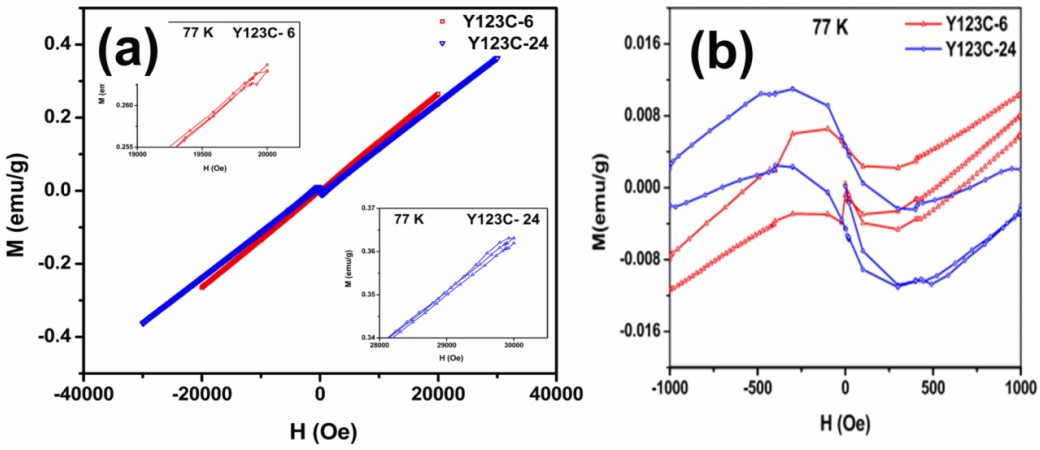

Figure 5. M-H loops obtained at 77 K. (a) the hysteresis loop recorded up to 2T and 3T for Y123C-6 and Y123C-24 respectively, and the inserts show that loops are not closed up to 2T and 3T respectively. (b) M-H loops recorded up to 1 kOe for the both the samples are shown.

Origin of ferromagnetism in nanoparticles of inorganic material is due to various reasons like the formation of cation or anion vacancies and surface effects, which varies from material to material. Particle surfaces, the associated changes and electronic states of the surface must play a primary and important role in the development of ferromagnetic behavior [12,14]. The M(H) curves for Y123C-6 and Y123C-24 were measured at temperatures 90 K to 300 K in applied fields of ±1 T are shown in Figure 6. Both the samples exhibit ferromagnetic behavior above T_c. Y123C-6 sample show higher magnetic moment than Y123C-24 and the ferromagnetic saturation moment coming down as the temperature increases for both the samples. In literature [20], there is a clear correlation between the size of the YBCO nanoparticles and the ferromagnetic feature of the particles. It is reported that the ferromagnetic moment decreases as the size of the particle increases due to diminished surface to volume ratio. The origin of ferromagnetism in YBCO particles is a surface effect similar to the reports in a variety of other metallic oxides which is due to the oxygen vacancy effects and the unsatisfied bonds in the surface region [13]. A muon resonance study on doped cuprates by Sonier et al. [51] indicates ferromagnetism in a heavily overdoped copper oxide superconductor. The present, approach produces Q1D YBCO without any additional dopant or excess phases. Hence, the occurrence of ferromagnetism in these samples can be understood through a different mechanism.

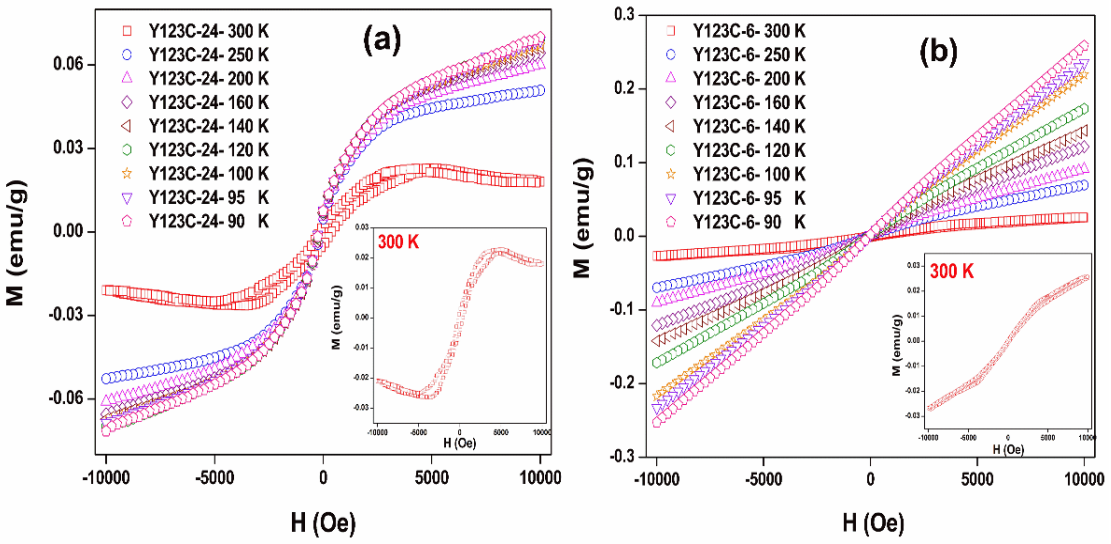

Figure 6. M-H loops recorded at different temperatures (90 K to 300 K) for Y123C-6 and Y123C-24 show ferromagnetic behavior. As shown in inserts the magnetic moment and hysteresis loops for Y123C-24 is larger than Y123C-6.

In the case of spin-triplet superconductors, such as UGe_2 the compatibility of ferromagnetism and superconductivity is not difficult to understand. YBCO are spin singlet superconductors where total spin is zero, the coexistence of these two orders is difficult to understand. Barbiellini and Jarlborg [52] suggested a possible explanation that ferromagnetism and superconductivity do not coexist uniformly but are phase-separated in nanodomains. In the present study, the coexistence of the ferromagnetism and superconductivity was not observed. Instead, as temperature decreased, the ferromagnetic moment decreased, and the behavior tend towards paramagnetism in both of the samples. The observation of ferromagnetism at room temperature occurring in nanoparticles of YBCO is of great interest and has significant implications. However, detailed studies are required to explore the presence or absence of ferromagnetism in the superconducting state.

4. Conclusion

We report the fabrication of fine nanometric sized single crystalline YBCO nano-rods from nitrate solution and cellulose. Nanorods were grown on micron sized YBCO particles when sintered for sufficiently long time. XRD results confirmed the formation of YBCO phase in both the Y123C-6 and Y123C-24 samples with a minor fraction of Ba-Cu-O phase. The increase in sintering time has favored YBCO phase at the expense of Ba-Cu-O phase. The single crystalline phase of YBCO nano-rods is confirmed through SAED measurement and compared with simulated SAED pattern. The diamagnetic transition below 90 K in M-T curves indicates the presence of superconductivity in both the samples. The width of the transition is broadened may be due to surface effects which are caused by the oxygen deficiency, inhomogeneity in the sample and (or) enhanced role of fluctuations in smaller sizes and loss of coordination at the surface. The M-H loops obtained on Y123C-6 and Y123C-24 are in agreement with the ferromagnetic behavior above T_c and with diamagnetic behavior below T_c. Oxygen deficiency in low dimensional YBCO system can increase the surface effects such as oxygen vacancies resulting in deterioration of the superconductivity and can favor room temperature

ferromagnetism in low dimension, but a distinctive understanding is yet to be devised. This opens up an innovative method of forming single crystalline YBCO nano-rods.

Acknowledgments

Authors thank IIT Hyderabad for PPMS facility. Mr. Mallesh, SEST, UoH is acknowledged for XRD measurements. Grant from XI plan, SoP, UoH is gratefully acknowledged for FE-SEM.

Conflict of Interest

The authors report no conflict of interests in this research.

References

1. Rao CNR, Kulkarni GU, Thomas PJ, et al. (2002) Size-Dependent Chemistry: Properties of Nanocrystals. *Chem A Eur J* 8: 28.
2. Ethayaraj M, Bandyopadhyaya R (2007) Mechanism and Modeling of Nanorod Formation from Nanodots. *Langmuir* 23: 6418.
3. Tachiki M, Yamashita T (1997) Sendai: Proc. 1st RIEC International Symposium on Intrinsic Josephson Effects and THz Plasma Oscillations in High-temperature Superconductors.
4. Bergeal N, Lesueur J, Sirena M, et al. (2007) Using ion irradiation to make high-T_c Josephson junctions. *J Appl Phys* 102: 083903.
5. Müller P, Festkörperprobleme À (1995) *Adv Solid State Phys* 34: 1.
6. Kleiner R, Müller P (1996) Critical Currents and Devices (New Age Int, India) 172.
7. Nagao M, Sato M, Maeda H, et al. (2003) Superconducting properties of single-crystal whiskers of $(Y_{0.86}Ca_{0.14})Ba_2Cu_3O_x$ $(Y_{0.86}Ca_{0.14})Ba_2Cu_3O_x$ grown from precursors containing calcium and tellurium. *Appl Phys Lett* 82: 1899–1901.
8. Yu AK, Golubev DS, Zaikin AD (2008) Superconductivity in one dimension Physics. *Reports* 464: 1-70.
9. Ginzburg V (1957) Ferromagnetic Superconductors. *J Exp Theor Phys* 4: 153.
10. Saxena SS, Agarwal P, Ahilan K, et al. (2000) Superconductivity on the border of itinerant-electron ferromagnetism in UGe_2, Superconductivity on the border of itinerant-electron ferromagnetism in UGe_2. *Nature* 406: 587.
11. Gasmia M, Khene S, Fillion G (2013) J Coexistence of superconductivity and ferromagnetism in nanosized YBCO powders. *J Phys Chem Solids* 74: 1414.
12. Sundaresan A, Rao CNR (2009) Ferromagnetism as a universal feature of inorganic nanoparticles. *Nano Today* 4: 96.
13. Shipra A, Gomathi A, Sundaresan A, et al. (2007) Room-temperature ferromagnetism in nanoparticles of superconducting materials. *Solid State Commun* 142: 685.
14. Sundaresan A, Rao CNR (2009) Implications and consequences of ferromagnetism universally exhibited by inorganic nanoparticles. *Solid State Commun* 149: 1197.
15. Sundaresan A, Bhargavi R, Rangarajan N, et al. (2006) Ferromagnetism as a universal feature of nanoparticles of the otherwise nonmagnetic oxides. *Phys Rev B* 74: 161306.
16. Elfimov IS, Yunoki S, Sawatzky GA (2002) Possible Path to a New Class of Ferromagnetic and Half-Metallic Ferromagnetic Materials. *Phys Rev Lett* 89: 216403.

17. Zywietz A, Furthmuller J, Bechstedt F (2000) Spin state of vacancies: From magnetic Jahn-Teller distortions to multiplets. *Phys Rev B* 62: 6854.
18. Hasanain SK, Akhtar N, Mumtaz A (2010) Particle size dependence of the superconductivity and ferromagnetism in YBCO nanoparticles. *J Nanoparticle Res* 13: 1953.
19. Alikhanzadeh Arani S, Salavati Niasari M (2011) Chemical Synthesis of Sub-Micrometer- to Nanometer-Sized of Antiferromagnetic Sr2CuO3 Ceramic. *Proceedings of the International Conference Nanomaterials: Applications and Properties*. 1: 1.
20. Arabi H, Jamshidi S, Komeili M, et al. (2013) Coexistence of Superconductivity and Ferromagnetic Phases in $YBa_2Cu_3O_{7-\delta}$Nanoparticles. *J Supercond Nov Magn* 26: 2069.
21. Zhu Z, Gao D, Dong C, et al. (2012) Coexistence of ferromagnetism and superconductivity in YBCO nanoparticles. *Phys Chem Chem Phys* 14: 3859.
22. Zhang YF, Tang YH, Duan XF, et al. (2000) Yttrium–barium–copper–oxygen nanorods synthesized by laser ablation. *Chem Phys Lett* 323: 180.
23. Zuo JM, Mabon JC (2004) Web-based Electron Microscopy Application Software: Web-EMAPS. *Microsc Microanal* 10. Available from: http://emaps.mrl.uiuc.edu/.
24. Martirosyan KS, Galstyan E, Xue YY, et al. (2008) The fabrication of YBCO superconductor polycrystalline powder by CCSO. *Supercond Sci Technol* 21: 065008.
25. Pathak LC, Mishra SK (2005) A review on the synthesis of Y–Ba–Cu-oxide powder. *Supercond Sci Technol* 18: R67.
26. Cava RJ, Batlogg B, Van Dover RB, et al. (1987) Bulk superconductivity at 91 K in single-phase oxygen-deficient perovskite $Ba_2YCu_3O_{9-\delta}$. *Phys Rev Lett* 58: 1676.
27. Bgreid TL, Fossheim K (1988) Evidence for Glasslike Dynamic Behaviour in $YBa_2Cu_3O_{7-}$x (YBCO) Superconductor. *Europhys Lett* 6: 81.
28. Mook HA, Dai P, Dogan F (2002) Charge and Spin Structure in $YBa_2Cu_3O_{6.35}$. *Phys Rev Lett* 88: 097004.
29. Mamalis AG, Petrov MI, Balaev DA, et al. (2001) A dc superconducting fault current limiter using die-pressed $YBa_2Cu_3O_7$ ceramic. *Supercond Sci Technol* 14: 413.
30. Maki K (1968) The Critical Fluctuation of the Order Parameter in Type-II Superconductors. *Prog Theor Phys* 39: 897.
31. Little WA (1967) Decay of Persistent Currents in Small Superconductors. *Phys Rev* 156: 396.
32. Zhang W-H, Sun Y, Zhang J-S, et al. (2014) Direct Observation of High-Temperature Superconductivity in One-Unit-Cell FeSe Films. *Chin Phys Lett* 31: 017401.
33. Giordano N (1988) Evidence for Macroscopic Quantum Tunneling in One-Dimensional Superconductors. *Phys Rev Lett* 61: 2137.
34. Zgirski M, Riikonen KP, Tuboltsev V, et al. (2005) Size Dependent Breakdown of Superconductivity in Ultranarrow Nanowires. *Nano Lett* 5: 1029.
35. Zgirski M, Riikonen KP, Tuboltsev V, et al. (2008) Quantum fluctuations in ultranarrow superconducting aluminum nanowires. *Phys Rev B* 77: 054508.
36. Altomare F, Chang AM, Melloch MR, et al. (2006) Evidence for Macroscopic Quantum Tunneling of Phase Slips in Long One-Dimensional Superconducting Al Wires. *Phys Rev Lett* 97: 017001.
37. Tian M, Kumar N, Xu S, et al. (2005) Suppression of Superconductivity in Zinc Nanowires by Bulk Superconductors. *Phys Rev Lett* 95: 076802.
38. Tian M, Wang J, Zhang Q, et al. (2009) Superconductivity and Quantum Oscillations in Crystalline Bi Nanowire. *Nano Lett* 9: 3196.

39. Wang J, Sun Y, Tian M, et al. (2012) Superconductivity in single crystalline Pb nanowires contacted by normal metal electrodes. *Phys Rev B* 86: 035439.
40. Bezryadin A, Lau CN, Tinkham M (2009) Quantum suppression of superconductivity in ultrathin nanowires. *Nature* 404: 971.
41. Bollinger AT, Reached A, Bezryadin A (2006) Dichotomy in short superconducting nanowires: Thermal phase slippage vs. Coulomb blockade. *Europhys Lett* 76: 505.
42. Sharifi F, Herzog AV, Dynes RC (1993) Crossover from two to one dimension in in situ grown wires of Pb. *Phys Rev Lett* 71: 428.
43. Rogachev A, Bezryadin A (2003) Superconducting properties of polycrystalline Nb nanowires templated by carbon nanotubes. *Appl Phys Lett* 83: 512.
44. Rogachev A, Bollinger AT, Bezryadin A (2005) Influence of High Magnetic Fields on the Superconducting Transition of One-Dimensional Nb and MoGe Nanowires. *Phys Rev Lett* 94: 017004.
45. Tian M, Wang J, Kurtz J S, et al. (2005) Dissipation in quasi-one-dimensional superconducting single-crystal Sn nanowires. *Phys Rev B* 71: 104521.
46. Michotte S, Piraux L, Boyer F, et al. (2004) Development of phase-slip centers in superconducting SnSn nanowires. *Appl Phys Lett* 85: 3175.
47. Piraux L, Encinas A, Vila L, et al. (2005) Magnetic and Superconducting Nanowires. *Nanosci Nano Technol* 5: 372.
48. Lukens JE, Warburton RJ, Webb WW (1970) Onset of Quantized Thermal Fluctuations in One-Dimensional Superconductors. *Phys Rev Lett* 25: 1180.
49. Newbower RS, Beasley MR, Tinkham M (1972) Fluctuation Effects on the Superconducting Transition of Tin Whisker Crystals. *Phys Rev B* 5: 864.
50. Muralt P, Pohl DW (1986) Scanning tunneling potentiometry. *Appl Phys Lett* 48: 514.
51. Soniera JE, Kaisera CV, Pacradounia V, et al. (2010) Direct search for a ferromagnetic phase in a heavily overdoped nonsuperconducting copper oxide. *P Natl Acad Sci* 107: 17131.
52. Barbiellini B, Jarlborg T (2008) Evidence for Macroscopic Quantum Tunneling of Phase Slips in Long One-Dimensional Superconducting Al Wires. *Phys Rev Lett* 101: 157002.

AIMS Press